J Toxicol Pathol 2022; 35: 183–192

Original Article

Elevated level of microRNA-210 at the initiation of muscular regeneration in acetic acid-induced non-ischemic skeletal muscular injury in mice

Yuichi Takai[1*], Takeshi Watanabe[1], and Tomoya Sano[1]

[1] Drug Safety Research and Evaluation, Takeda Pharmaceutical Company Limited, 26-1 Muraoka-Higashi 2 Chome, Fujisawa, Kanagawa 251-8555, Japan

Abstract: The alteration in microRNA-210 level, a hypoxia-inducible microRNA, is not well known in non-ischemic tissue injury. In this study, we characterized the histopathological time course of acetic acid-induced skeletal muscle injury as a non-ischemic tissue injury model and investigated the expression of microRNA-210, hypoxia-inducible factor 1α, and growth factors using quantitative polymerase chain reaction analysis. After a single intramuscular dose of 3% (v/v) acetic acid to C57BL/6J mice, focal coagulative necrosis of muscle fibers was noted from 3 h after dosing and infiltration of F4/80 and Galectin-3 positive M2 macrophage was noted at 1 d after dosing. Muscular regeneration was initiated from 3 d, when M2 macrophage infiltration was most prominent, till 14 d after dosing. *Hif1α* and *Hgf* expression increased from 3 h onwards, and microRNA-210 level increased after 3 d after the treatment. However, no clear elevation in the levels of *Igf1* or *Vegf* was observed. The infiltrative macrophages and regenerative muscle fibers were positive for hypoxia-inducible factor 1α, microRNA-210, and hepatocyte growth factor as assessed by immunohistochemistry or *in situ* hybridization. In this study, dominant infiltration of M2 macrophages at muscular necrosis and subsequent regeneration after a single intramuscular injection of acetic acid in mice were observed. The increase in hif1α level was observed just after the muscular injury in this non-ischemic tissue injury model, and the elevation in microRNA-210 level was noted at the initiation of tissue regeneration, indicating its effects on tissue protection and repair. (DOI: 10.1293/tox.2021-0061; J Toxicol Pathol 2022; 35: 183–192)

Key words: acetic acid, hypoxia-inducible factor 1α, microRNA-210, macrophage, regeneration, mice

Introduction

The expression of hypoxia-inducible factor (HIF) is upregulated under hypoxic conditions[1, 2]. Upon the expression of HIF, several microRNAs (miRNAs) are upregulated and miR-210 is one of the major hypoxia-inducible miRNAs[1]. miRNA-210 is reported to be highly expressed under hypoxic conditions, such as in the cardiovascular system[3], brain[4], skin[5, 6], and tumor tissues[1], and increased miRNA-210 expression was observed in a peripheral ischemic mouse skeletal muscular injury model[7]. In our previous study, miRNA-210 expression was observed in myoblasts and macrophages 3 days after ischemic muscular injury, indicating its association with muscular regeneration[7]. Zaccagnini *et al.* have reported that miRNA-210 inhibition increased ischemic tissue damage, and miRNA-210 overexpression attenuated tissue damage and the inflammatory response with a reduced number of infiltrative macrophages after hindlimb ischemia[8, 9]. Interestingly, miRNA-210 expression increases during myogenic differentiation under normoxia with an HIF-1α dependent mechanism in *in vitro* conditions[10]. In addition, miRNA-210 elevation has been reported in the regeneration phase after cardiotoxin-induced muscular injury in mice[10]. Therefore, the elucidation of HIF-1α and miRNA-210 expression profiles in non-ischemic muscular injury is important to further understand their biological significance.

Several skeletal muscular injury models have been developed to study skeletal muscle repair and regeneration[11–15]. However, volumetric muscle loss and mechanical trauma models require validation by a surgical procedure or establishment of a drop-tower device for trauma under anesthesia[11–14]. Cardiotoxin-induced muscular injury can be simply reproduced by intramuscular injection[15]. However, protein kinase C (PKC) inhibition is known to be one of the pharmacological actions of the cardiotoxin[16], and PKC zeta plays an important role in HIF-1α activation[17]. To avoid the possible pharmacological effect of the cardiotoxin on HIF-1α, we chose acetic acid in this study as an alternative chemical to induce non-ischemic muscular injury model[18, 19], which can be reproduced with intramuscular injection.

Received: 15 September 2021, Accepted: 29 November 2021
Published online in J-STAGE: 24 December 2021
*Corresponding author: Y Takai (e-mail: yuuichi.takai@takeda.com)

In the present study, we investigated the detailed histopathological time course in a mouse model of acetic acid-induced muscular injury by profiling HIF-1α and miRNA-210 expression. In addition, we investigated the expression of growth factors, such as hepatocyte growth factor (HGF), insulin-like growth factor (IGF)-1, and vascular endothelial growth factor (VEGF), since these growth factors are considered to be related to muscle homeostasis and regeneration[20–22] and HGF and VEGF can be upregulated by HIF-1α[23, 24].

Materials and Methods

Six-week-old male C57BL/6J mice purchased from Charles River Laboratories Japan, Inc. (Tokyo, Japan) were used in this study. Twenty animals were maintained on a laboratory chow diet (CE-2, CLEA Japan, Inc., Tokyo, Japan) and allowed free access to water and food before and during the experiments. The care and use of the animals as well as the experimental protocols used in this study were approved by the Institutional Animal Care and Use Committee of Takeda Pharmaceutical Co., Ltd. (approval code: 00020216).

Animal model of muscular injury with acetic acid

We used acetic acid, a well-known irritative agent[18], for inducing the skeletal muscle injury model in this study. The animals were administered 3% (v/v) acetic acid (Wako, Osaka, Japan) diluted with saline intramuscularly at 50 μL/site into the left side of the gastrocnemius. Four animals per time point were euthanized at 3 h and 1, 3, 7, and 14 d after acetic acid administration. After necropsy, both sides of the gastrocnemius were removed, trimmed, and fixed in 10% (v/v) neutral buffered formalin (NBF). Portions of the gastrocnemius muscles were immersed in RNAlater (Ambion, Inc., Austin, TX, USA) for 24 h in a refrigerator and preserved at −20°C until quantitative polymerase chain reaction (qPCR) analysis. The acetic-acid-related effects were determined through a comparison with the non-treated gastrocnemius muscles (right side) as a control. After fixation in NBF, the gastrocnemius muscles were embedded in paraffin, sectioned transversely, and stained with hematoxylin and eosin (H&E). Using sequential sections, immunohistochemistry (IHC) for F4/80, iNOS, and galectin-3 (Gal-3) as pan-, M1, and M2 macrophage markers, respectively[25, 26], were carried out for all samples showing cellular infiltration in H&E sections, for macrophage characterization. For the interpretation of the qPCR results, IHC for HIF-1α and HGF and *in situ* hybridization (ISH) for miRNA-210 were performed with representative samples obtained at 3 d after the administration of acetic acid. The IHC staining conditions for each primary antibody are summarized in Table 1. ISH was carried out according to the instruction manual v3.0 of the miRCURY LNA™ microRNA ISH Optimization Kit (FFPE) developed by Exiqon (Vedbaek, Denmark) with minor modifications. We used digoxigenin (DIG)-labeled locked nucleic acid (LNA)-modified probes for miRNA-210 (hsa-miR-210, Product. No. 18103-15), positive control (U6 snRNA, product. No. 90010), and negative control (scrambled microRNA, Product. No. 90010) from Exiqon. After deparaffinization, proteinase-K (Exiqon: Product No. 90010, miRCURY LNA; microRNA Detection, control probes, buffer, and ProtK) at 10 μg/mL was incubated at 37 °C for 13 min. After washing with PBS, the LNA-probes, namely miRNA-210 (400 nM), scramble-miRNA (400 nM), and U6 (1 nM), were hybridized at 60 °C for 60 min. After immersion in 5 × SSC buffer at room temperature, the specimens were washed in pre-heated SSC buffer (55 °C), 1 × 5 min in 5 × SSC, 2 × 5 min in 1 × SSC, 2 × 5 min in 0.2 × SSC, and finally 1 × 5 min in 0.2 × SSC at room temperature and then immersed in PBS. Sections were blocked against non-specific binding in blocking solution composed of 2% (v/v) sheep serum and 1% (v/v) bovine serum albumin in PBS-T for 15 min at room temperature (RT). Alkaline phosphatase (AP)-conjugated anti-DIG (Product No. 11093274910, Roche, Mannheim, Germany) (1:200) was incubated for 60 min at RT for immunological detection. After washing with PBS-T, the substrate enzymatic reaction was carried out with NBT/BCIP (Product No. 1697471001, Roche) at 30 °C for 2 h. The reaction was stopped with a 2 × 5 min wash in KTBT buffer (50 mM Tris–HCl, 150 mM NaCl, and 10 mM KCl). Sections were counterstained with Nuclear Fast Red at room temperature for 3 min and then rinsed with tap water. After dehydration by increasing the gradient of the

Table 1. Primary Antibodies and Reaction Conditions for immunohistochemistry

Antibody	Host	Clonality	Supplier	Dilution	Antigen retrieval	Detection system
F4/80	Rat	mono: CI:A3-1	Gene Tex (GTX26640)	×500	Trypsin, 37°C, 10 min	Histofine® Simple Stain™ Mouse MAX PO (Rat)
iNOS	Rabbit	mono: SP126	Abcam (Ab115819)	×100	Trypsin, 37°C, 10 min	Histofine® Simple Stain™ Mouse MAX PO (R)
Gal-3	Rat	mono: M3/38	CEDARLANE (CL8942AP)	×5,000	-	Histofine® Simple Stain™ Mouse MAX PO (Rat)
HIF-1α	Mouse	mono: H1α67	Calbiochem (400080)	×500	Immersed in citric buffer (pH6) in AC, 121°C, 10 min	Histofine® MOUSESTAIN KIT
HGF	Goat	poly	R&D SYSTEMS (AF2207)	×100	Immersed in citric buffer (pH6) in MW (700W), 5 min	Histofine® Simple Stain™ Mouse MAX PO (G)

AC: autoclave; MW: microwave; mono: monoclonal; poly: polyclonal.

ethanol solutions, the specimens were mounted with Permount (Fisher Scientific Inc., Pittsburgh, PA, USA).

mRNA and miRNA quantification

For relative quantification of *Hif1α*, *Hgf*, *Igf1*, *Vegf*, and miRNA-210 using the comparative Ct method ($2^{-\Delta\Delta Ct}$), qPCR was conducted with all animal samples after extraction of total RNA and reverse transcription to complementary DNA (cDNA). Total RNA was extracted from cryopreserved muscle samples using the miRNeasy Mini Kit (Product No. 217004, QIAGEN, Hilden, Germany). Reverse transcription of cDNA for mRNA and miRNA quantification was carried out using the SuperScript VILO cDNA Synthesis Kit (Product No. 11754-250, Thermo Fisher Scientific, Waltham, MA, USA) and Universal cDNA Synthesis Kit II (Product No. 203301, Exiqon), respectively. Subsequently, the relative mRNA levels of Hif1a, *Hgf*, *Igf1*, and *Vegf* (probe product Nos.: Mm00468869_m1, Mm01135184_m1, Mm00439560_m1, and Mm00437306_m1, respectively; Thermo Fisher Scientific) were analyzed using TaqMan Fast Advanced Master Mix (Product No. 4444557, Thermo Fisher Scientific) with TATA-binding protein as a reference gene (Probe product No. Mm01277042_m1; Thermo Fisher Scientific), while the relative miRNA-210 expression levels (hsa-miR-210, Probe product No. 204333; Exiqon) were analyzed using ExiLENT SYBR Green master mix (Product No. 203402, Exiqon) with miRNA-191-5p as a reference miRNA (has-miR-191-5p, Probe product No. 204306, Exiqon). All PCR procedures were conducted using a 7900 HT Fast Real-Time PCR System (Applied Biosystems, Foster City, CA, USA).

The qPCR data for miRNANA and mRNA were tested by the F-test for homogeneity of variance between the non-treatment and treatment sides. When the variances were homogeneous, Student's t-test was used, and when the variances were heterogeneous, Aspin–Welch t-test was performed to compare the mean of the control group with that of the dosage group[27]. The F-test was conducted at a significance of 0.20, and the other tests were conducted at two-tailed significance levels of 0.05, 0.01, and 0.001. Statistical analyses were performed using SAS version 9.3 (SAS Institute Inc., Cary, NC, USA).

Results

Histopathology and IHC for macrophage markers (F4/80, iNOS, and Gal-3)

After a single intramuscular dose of 3% (v/v) acetic acid, focal necrosis/degeneration of muscle fibers was noted at the injection site after 3 h, which progressed to coagulation necrosis thereafter. Its severity was prominent at 1 and 3 d and decreased at 7 and 14 d after administration. The other findings mentioned below were located adjacent to the necrotic area. The regeneration of the muscle fiber was observed at 3 d after the administration of acetic acid with the appearance of basophilic myoblasts and at 7 and 14 d with the central nucleus fibers. Minimal neutrophil infiltration (only in one animal) and minimal to mild mononuclear cell infiltration were observed in the interstitial tissue around the necrotic area from 3 h; its severity and/or incidence increased over time and were most prominent at 3 d when minimal neutrophil and mild mononuclear cell infiltration around necrosis were noted in all animals. The main component of the infiltrated cells at 7 and 14 d after the administration of acetic acid was mononuclear cells. Most infiltrative mononuclear cells were positive for F4/80 (a pan-macrophage marker) and Gal-3 (M2 macrophage marker) throughout the experimental period, and their distributions were almost comparable. On the other hand, no positive reaction for iNOS (M1 macrophage marker) was noted from 3 h to 1 d. Only some mononuclear cells were positive for iNOS from 3 d to 14 d, but they were a minor component in comparison to the F4/80- and Gal-3-positive cells. These immunohistochemical results suggested M2 dominant macrophage infiltration throughout the study period. A few animals showed minimal hemorrhage in and around the necrotic area focally at 1 and 7 d, but no other findings indicating circulatory impairment, such as vascular injury, were noted in the intact area of the treated muscle. Interstitial fibrosis was noted at 3 d and thereafter, and the incidence was high at 7 and 14 d (Figs. 1 and 2; Tables 2 and 3).

Expressions of HIF-1α and miRNA-210

The qPCR data showed that the gene expression of *Hif1α* in the treated muscles was higher than that in the non-treated muscles, with statistically significant difference from 3 h to 7 d after the administration of acetic acid, and was prominent from 3 h to 3 d after the treatment. A statistically significant increase in *Hif1α* expression was also noted at 14 d but was not considered to indicate pathophysiological significance since the extent of increase was small (less than 1.5 times higher). A statistically significant increase in the expression of miRNA-210 was observed only at 3 d after the treatment (Fig. 3).

IHC and ISH showed comparable positive reactions of HIF-1α and miRNA-210 in the cytoplasm of macrophages and regenerative muscle fibers, myoblasts, around the necrotic area at 3 d after the treatment (Fig. 4). Positive reactions were not observed in the intact muscle fibers.

Expressions of growth factors: HGF, IGF-1, and VEGF

The gene expression of *Hgf* in the treated muscles was significantly higher than that in the non-treated muscles throughout the experimental period, and was prominent (more than a 10-fold increase) at 3 d after the treatment. The gene expression of *Vegf* decreased from 1 d to 7 d after the treatment, which was statistically significant. Although a statistically significant increase in *Vegf* expression was noted at 3 h, it was not pathophysiologically significant (approximately 1.2 times higher). No statistically significant changes were noted in *Igf1* expression throughout the experimental period, although it tended to increase at 7 and 14 d after the treatment (Fig. 3).

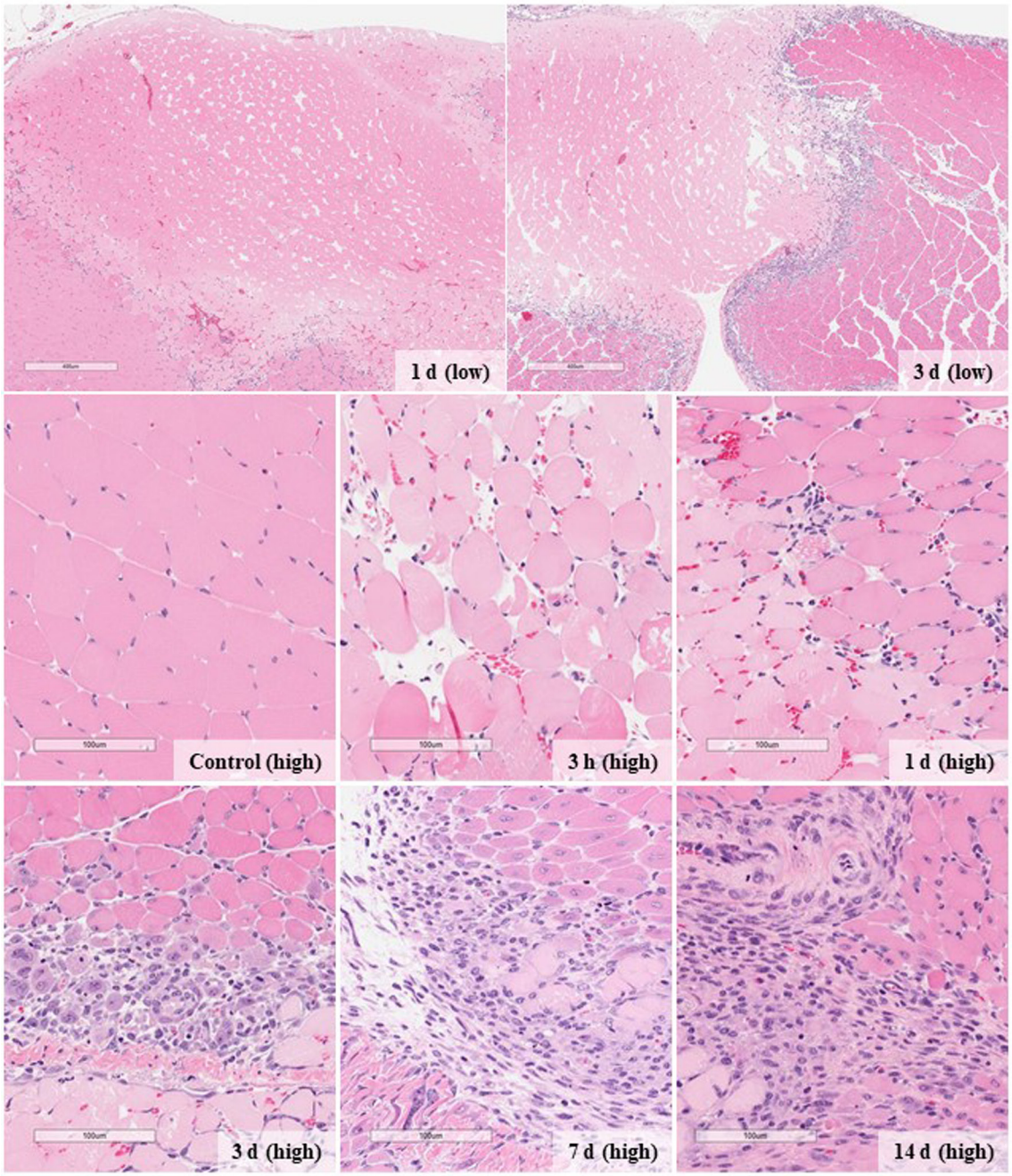

Fig. 1. Low magnification images (labeled as low) show the distribution of moderate focal coagulation necrosis of muscle fibers in acetic acid-induced muscular injury model at 1 and 3 d. Bar=400 μm. Images in the middle and lower panels show the time course of the histological features from control and 3 h to 14 d after the treatment at high magnification (labeled as high). Bar=100 μm.

Immunohistochemical signals of HGF were observed in macrophages and myoblasts at 3 d after the treatment, which was consistent with the distribution of HIF-1α and miRNA-210 (Fig. 4). Immunohistochemical signals were not observed in the intact muscle fibers.

Discussion

In this study, focal muscular necrosis/degeneration was observed a few hours after a single intramuscular administration of acetic acid in mice, which eventually progressed to coagulation necrosis. Its severity was prominent at 1 and 3 d after the treatment. Muscular regeneration with the appearance of basophilic myoblasts was initiated 3 d after the

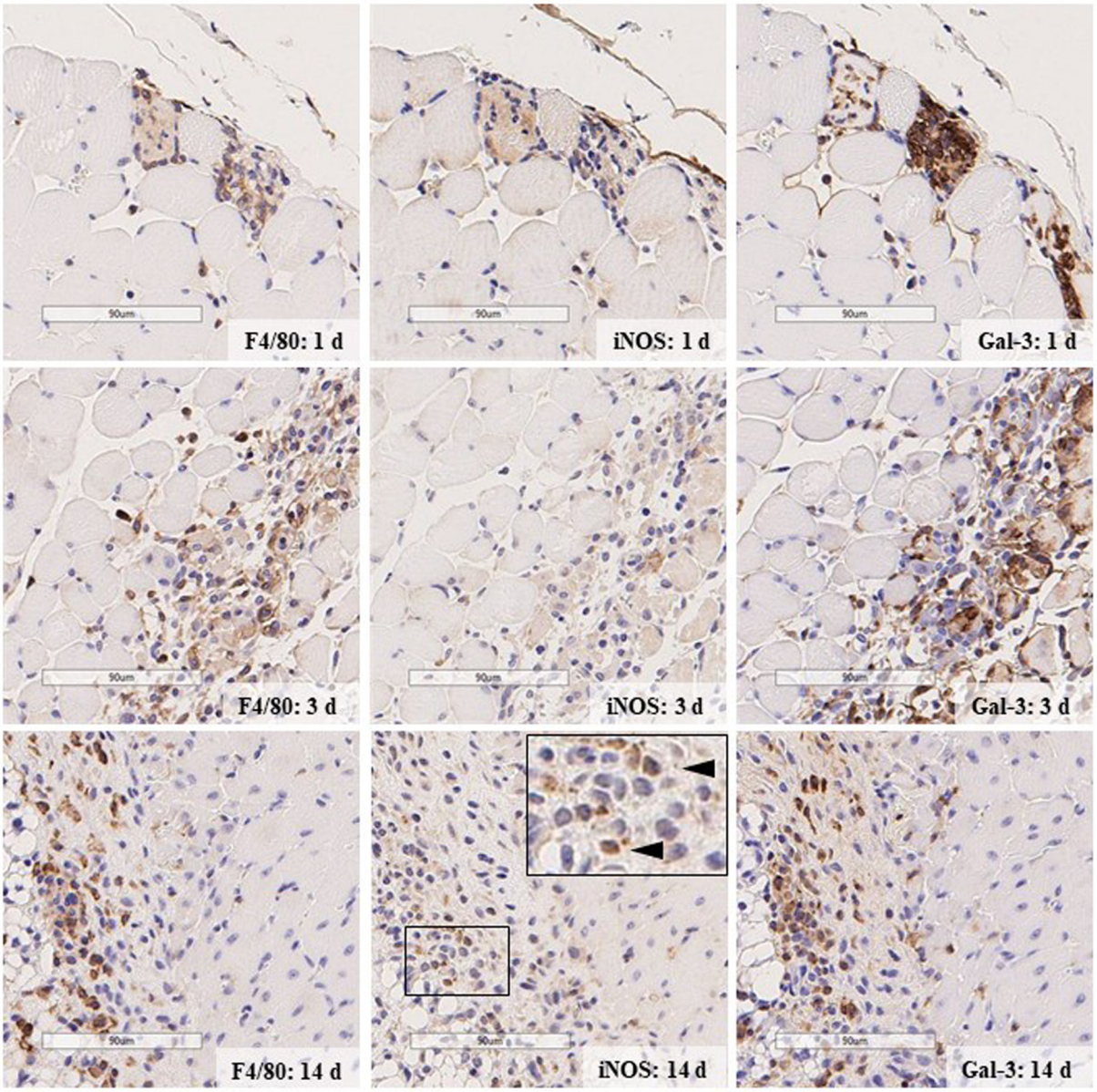

Fig. 2. Immunohistochemistry of F4/80, iNOS, and Gal-3 at 1, 3, and 14 d after the treatment, respectively. Arrowheads show iNOS-positive cells at 14 d. Bar=90 μm.

treatment. Macrophage infiltration was observed in the interstitial tissue from tissue injury to the recovery process, which was the most prominent 3 d after the treatment. In general, infiltrative macrophages are categorized into pro-inflammatory M1 and anti-inflammatory M2 phenotypes[26]. In skeletal muscle injury, M1 macrophages infiltrate early to promote the clearance of necrotic debris during the inflammation phase shortly after neutrophil infiltration, whereas M2 macrophages appear later to sustain tissue healing[28] Notably, the pattern of macrophage infiltration among the injury models seemed to vary. Martins *et al.* have reported M1 macrophage infiltration just after traumatic injury that slowly increased over time until 15 d after the treatment, and M2 macrophage infiltration peaked at 4 d after the treatment[14]. In the cardiotoxin-induced model, Bouredji *et al.* showed M1 and M2 macrophage infiltration at 3 d after the treatment, with a tendency to decrease and increase, respectively at 7 d[29]. However, in the acetic acid-induced muscular injury, neither prominent M1 macrophage infiltration nor neutrophilic infiltration was observed, and most of the infiltrative macrophages were of the M2 phenotype.

As assessed by qPCR, *Hif1α* elevation was prominent from 3 h to 3 d after the treatment and remained until 7 d, which was consistent with the severity of muscular necrosis. On the other hand, miRNA-210 increased transiently at 3 d after the treatment, when macrophage infiltration was most prominent and muscular regeneration was initiated, and the elevated levels returned to the baseline at 7 d. In IHC or

Table 2. Incidence and Severity of the Histopathological Findings in the Muscle Tissue after a Single Dose of Acetic Acid

Findngs/Grade	3 hours	1 day	3 days	7 days	14 days
Focal necrosis/degeneration of muscle fibers	4/4	4/4	4/4	3/4	2/4
Minimal	1	1	0	2	2
Mild	3	1	1	1	0
Moderate	0	2	3	0	0
Regeneration of muscle fibers	0/4	0/4	4/4	4/4	4/4
Minimal	-	-	4	4	4
Neutrophil infiltration	1/4	4/4	4/4	0/4	0/4
Minimal	1	4	4	-	-
Mononuclear cell infiltration	0/4	4/4	4/4	4/4	4/4
Minimal	-	4	0	4	4
Mild	-	0	4	0	0
Fibrosis	0/4	0/4	1/4	4/4	3/4
Minimal	-	-	1	4	3
Hemorrhage	0/4	2/4	0/4	1/4	0/4
Minimal	-	2	-	1	-

No noteworthy findings were noted in the muscle of non-treatment side in any animal.
The incidence of each finding was described as "animal number with each finding" / "animal number examined".
Focal necrosis/degeneration of muscle fibers observed at 3 h progressed to coagulation necrosis thereafter.

Table 3. Incidence and Severity of Immunohistochemistry for F4/80, INOS, and Gal-3 in Infiltrative Cells

Grade		F4/80					iNOS					Gal-3				
		3h	1d	3d	7d	14d	3h	1d	3d	7d	14d	3h	1d	3d	7d	14d
-:	Negative	0	0	0	0	0	1	4	3	2	0	0	0	0	0	0
+/-:	Some mononuclear cells were positive.	1	0	0	0	0	0	0	1	2	4	1	0	0	0	0
+:	Approximately 10 to 30% of mononuclear cells were positive.	0	3	0	0	2	0	0	0	0	0	0	0	0	0	2
++:	Approximately 30 to 60% of mononuclear cells were positive.	0	1	1	0	1	0	0	0	0	0	0	4	0	0	1
+++:	More than 60% of mononuclear cells were positive.	0	0	3	4	1	0	0	0	0	0	0	0	4	4	1

All amnimals which showed interstitial cell infiltration were examined: N=1 at 3 hours, N=4 from 1 to 14 d.
Histopathological finidngs and grades are as below. Minimal neutrophil infiltration at 3 h to 3 d, mild mononuclear cell infiltration at 3 d, minimal mononuclear cell infiltration at 1, 7 and 14 d.

ISH staining, positive reactions of HIF-1α and miRNA-210 were observed in the cytoplasm of infiltrative macrophages and regenerative muscle fibers around the time of necrosis at 3 d after treatment. The comparable histological distribution indicated that miRNA-210 elevation was induced in a HIF-1α-dependent manner. It has been reported that HIF-1α-dependent miRNA-210 induction was observed in murine macrophages[30] and myoblasts[10] under normoxic *in vitro* conditions. The increased expression of HIF-1α was considered to be induced by muscular necrosis or possibly by acidic conditions after acetic acid injection as HIF-1α can be activated when it comes in contact with cell debris derived from myotubes or low pH conditions independent of hypoxia[31, 32]. Moreover, in this study, the existence of muscular necrosis/degeneration and a few cases of minimal hemorrhage indicated the possibility of focal hypoxia, which could be partially related to the increased expression of *Hif1α*. However, its contribution was considered less dominant than that observed in the hindlimb ischemia model, wherein a severe reduction in blood flow was noted after arterial ligation[7], whereas no other histopathological findings indicating circulation impairment were noted in the intact area of the treated muscles in this study. Under hypoxic conditions, HIF-1α can continuously act as a transcriptional factor after transfer to the nucleus, and miRNA-210 expression can be upregulated thereafter[1, 33]. In the hindlimb ischemia model, significantly increased miRNA-210 expression was noted from 3 d to 14 d after femoral artery dissection using qPCR[8]. In contrast, in acetic acid-induced muscular injury, qPCR data showed that miRNA-210 increased transiently at 3 d, the timing of the initiation of muscular regeneration. The association between miRNA-210 expression and muscular regeneration was also demonstrated in the hindlimb ischemia model because increased miRNA-210 expression was noted in the myoblasts and macrophages during the muscular regenerative phase[7]; however, the transient miRNA-210 expression seen in the acetic acid-induced non-ischemic muscular injury model may suggest a more specific role of miRNA-210 expression in the process from muscular injury to regeneration. The elevated levels of miRNA-210 observed in this study may play anti-inflammatory or cytoprotective roles in the muscular tissue during the regeneration phase, as has also been demonstrated in the literature; for example, inhibition of NF-κB expression in macrophages followed by

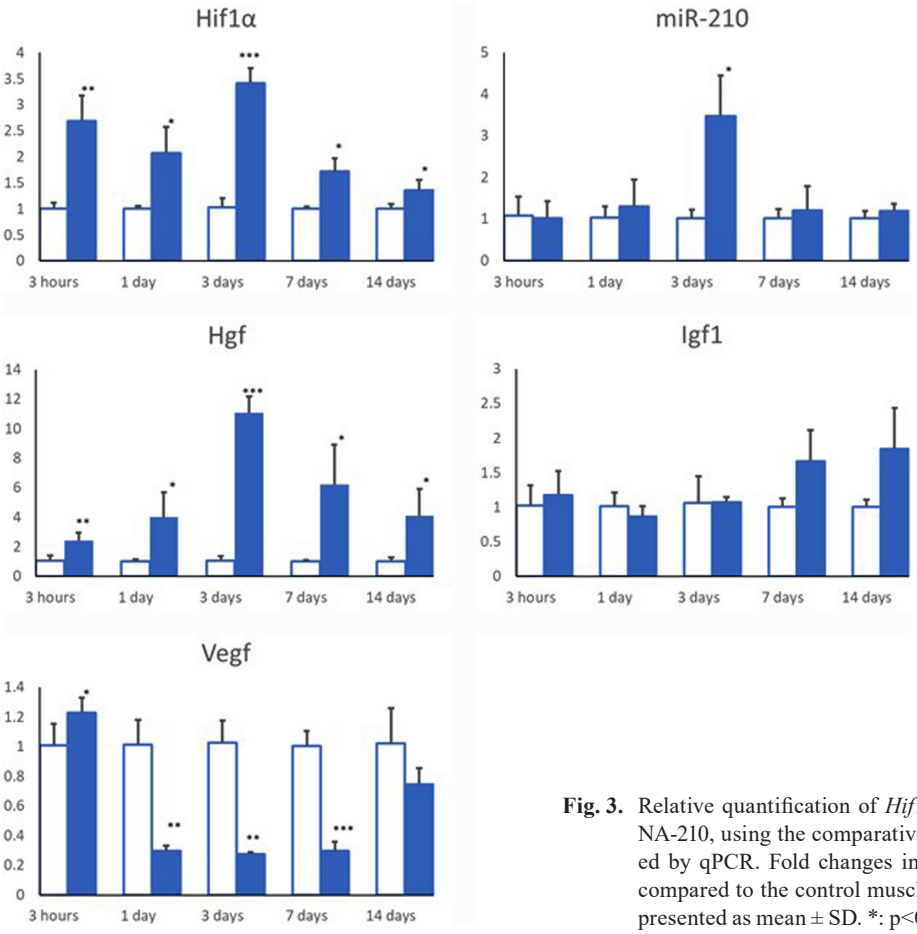

Fig. 3. Relative quantification of *Hif1α*, *Hgf*, *Igf1*, and *Vegf* and miRNA-210, using the comparative Ct method ($2^{-\Delta\Delta Ct}$) was conducted by qPCR. Fold changes in the treated muscle (blue bar) as compared to the control muscle (white bar) are shown. Data are presented as mean ± SD. *: $p<0.05$, **: $p<0.01$, and ***: $p<0.001$.

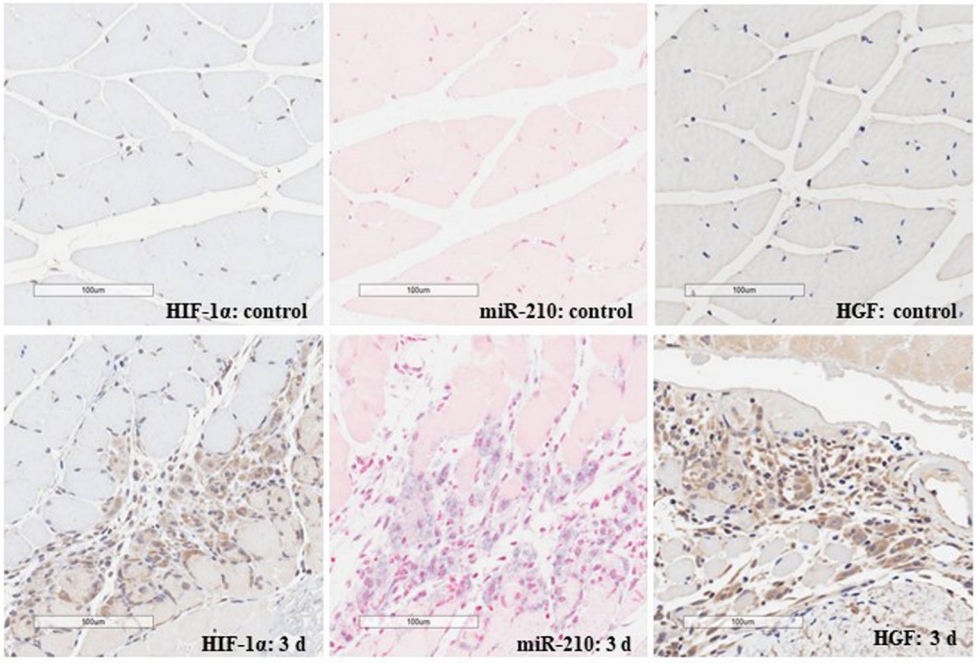

Fig. 4. Immunohistochemistry (IHC) or *in situ* hybridization (ISH) for HIF1α (IHC), miRNA-210 (ISH), and HGF (IHC), control and 3 d after the treatment. Bar=100 μm.

a decrease in TNF-α, IL-6, and iNOS[30], improved angiogenesis and tissue repair[9], and tissue-protective effects during myogenic differentiation of myoblasts[8, 10].

Increased growth factor expression has been observed after muscular injury or during the regeneration processes, such as an increase in HGF mRNA and protein expression during the regeneration from ischemic injury or muscular atrophy[34, 35], elevation in IGF-1 mRNA levels from tissue injury to regeneration phases after muscle contusion[36], and a transient increase in VEGF mRNA 12 h after a single freezing injury[37]. In the acetic acid-induced muscular injury, increased *Hgf* expression was noted throughout the experimental period, and its expression was most prominent at 3 d after the treatment. The increased *Hgf* level was considered to be a result of its expression in the infiltrative macrophages and regenerative muscle fibers based on the results of IHC for HGF.

HGF is secreted by M2 macrophages as a means of tissue repair[38], and its expression in the muscular tissue also exerts protective effects in muscular injury; HGF can increase the number of myoblasts in a damaged muscle tissue, but can also inhibit muscle differentiation[20]. Therefore, increased *Hgf* expression and the immunohistochemical results could be indicative of their roles in tissue repair in infiltrative macrophages and regenerative muscle fibers.

The expression of miRNA-210 in infiltrative macrophages and regenerative muscle fibers could be related to the expression of HGF, since increased expression of HGF was observed in acute myocardial infarction rat models who received miRNA-210 agonist[39]. In addition, HGF expression can be upregulated by HIF-1α under hypoxic *in vitro* condition[23], and our results showed a simultaneous increase in the expressions of *Hif1α* and *Hgf*.

Meanwhile, a clear elevation in the level of *Igf1* was not induced in this study, although a slight increase in *Igf1* was noted at 7 and 14 d after the treatment. Thus, there seemed to be some differences in the expression pattern of *Igf1* from that in other muscular injury models, although the underlying reasons remained unclear. In the muscle contusion or cardiotoxin-induced model, elevation in *Igf1* levels was observed from tissue injury to regeneration phases as a factor that affected the diameter of muscle fibers[36, 40, 41]. In particular, in cardiotoxin-induced muscular injury, macrophage-derived IGF-1 is considered a key factor in inflammation resolution and macrophage polarization during muscle regeneration[40]. Although we could not compare the degree of macrophage infiltration between the cardiotoxin-[40] and acetic acid-induced models, the possibility of low intensity of macrophage infiltration might be related to only a slight increase in *Igf1* level observed in this study.

It has been reported that *Vegf* expression can be upregulated by HIF-1α or miRNA-210 under hypoxic *in vitro* condition[24, 42]; however, *Vegf* expression was found to significantly decrease from 1 d to 7 d in this study. A similar decrease in *Vegf* expression in the muscle tissue was noted after 1 to 3 d after a single dose of cardiotoxin in heme oxiganase-1 knockout and wild type mice[41], despite reports of increased *Hif1α* or miRNA-210 expression levels in cardiotoxin-induced muscular injury[10, 43]. Ochoa *et al.* also showed a decrease in VEGF protein expression after 1 to 3 d of cardiotoxin-induced muscular injury[44]. Furthermore, they demonstrated that the decrease in VEGF expression was exacerbated and lasted until 14 d under CCR-dependent impairments of $F4/80^+$ macrophage infiltration[44].

In conclusion, dominant infiltration of M2 macrophages was confirmed in the area adjacent to the focal coagulation necrosis of muscle fibers, where following muscular regeneration was observed after a single intramuscular injection of acetic acid in mice. M1 macrophage or neutrophil infiltration was not prominent. An increase in the *Hif1α* level was observed from 3 h to 7 d after the treatment, and the elevations in miRNA-210 and *Hgf* levels were clearly noted at 3 d after the treatment at which tissue regeneration was initiated. miRNA-210, HIF-1α, and HGF were histologically detected in macrophages and myoblasts. These results indicate the tissue-protective and regenerative effects of miRNA-210 after muscular injury, independent of ischemia.

Disclosure of Potential Conflicts of Interest: The authors declare that there are no conflicts of interest associated with this manuscript.

Acknowledgment: The authors would like to thank Kenta Danbayashi and Yumiko Miyamoto from Axcelead Drug Discovery Partners Inc. for technical support with qPCR, IHC, and ISH, Tomomi Kaneyama from BoZo Research Center Inc. for technical support with IHC, and Shingo Okubo from Takeda Pharmaceutical Company Limited for reviewing the manuscript.

References

1. Chan YC, Banerjee J, Choi SY, and Sen CK. miR-210: the master hypoxamir. Microcirculation. **19**: 215–223. 2012. [Medline] [CrossRef]
2. Stroka DM, Burkhardt T, Desbaillets I, Wenger RH, Neil DA, Bauer C, Gassmann M, and Candinas D. HIF-1 is expressed in normoxic tissue and displays an organ-specific regulation under systemic hypoxia. FASEB J. **15**: 2445–2453. 2001. [Medline] [CrossRef]
3. Devlin C, Greco S, Martelli F, and Ivan M. miR-210: More than a silent player in hypoxia. IUBMB Life. **63**: 94–100. 2011. [Medline]
4. Lou YL, Guo F, Liu F, Gao FL, Zhang PQ, Niu X, Guo SC, Yin JH, Wang Y, and Deng ZF. miR-210 activates notch signaling pathway in angiogenesis induced by cerebral ischemia. Mol Cell Biochem. **370**: 45–51. 2012. [Medline] [CrossRef]
5. Chang KP, and Lai CS. Micro-RNA profiling as biomarkers in flap ischemia-reperfusion injury. Microsurgery. **32**: 642–648. 2012. [Medline] [CrossRef]
6. Biswas S, Roy S, Banerjee J, Hussain SR, Khanna S, Meenakshisundaram G, Kuppusamy P, Friedman A, and Sen CK. Hypoxia inducible microRNA 210 attenuates keratinocyte proliferation and impairs closure in a murine model of isch-

emic wounds. Proc Natl Acad Sci USA. **107**: 6976–6981. 2010. [Medline] [CrossRef]
7. Takai Y, Nishimura S, Kandori H, and Watanabe T. Histopathological significance of microRNA-210 expression in acute peripheral ischemia in a murine femoral artery ligation model. J Toxicol Pathol. **33**: 211–217. 2020. [Medline] [CrossRef]
8. Zaccagnini G, Maimone B, Di Stefano V, Fasanaro P, Greco S, Perfetti A, Capogrossi MC, Gaetano C, and Martelli F. Hypoxia-induced miR-210 modulates tissue response to acute peripheral ischemia. Antioxid Redox Signal. **21**: 1177–1188. 2014. [Medline] [CrossRef]
9. Zaccagnini G, Greco S, Longo M, Maimone B, Voellenkle C, Fuschi P, Carrara M, Creo P, Maselli D, Tirone M, Mazzone M, Gaetano C, Spinetti G, and Martelli F. Hypoxia-induced miR-210 modulates the inflammatory response and fibrosis upon acute ischemia. Cell Death Dis. **12**: 435. 2021. [Medline] [CrossRef]
10. Cicchillitti L, Di Stefano V, Isaia E, Crimaldi L, Fasanaro P, Ambrosino V, Antonini A, Capogrossi MC, Gaetano C, Piaggio G, and Martelli F. Hypoxia-inducible factor 1-α induces miR-210 in normoxic differentiating myoblasts. J Biol Chem. **287**: 44761–44771. 2012. [Medline] [CrossRef]
11. Sicherer ST, Venkatarama RS, and Grasman JM. Recent trends in injury models to study skeletal muscle regeneration and repair. Bioengineering (Basel). **7**: 76. 2020. [Medline]
12. Xu P, Werner JU, Milerski S, Hamp CM, Kuzenko T, Jähnert M, Gottmann P, de Roy L, Warnecke D, Abaei A, Palmer A, Huber-Lang M, Dürselen L, Rasche V, Schürmann A, Wabitsch M, and Knippschild U. Diet-induced obesity affects muscle regeneration after murine blunt muscle trauma—a broad spectrum analysis. Front Physiol. **9**: 674. 2018. [Medline] [CrossRef]
13. Werner JU, Tödter K, Xu P, Lockhart L, Jähnert M, Gottmann P, Schürmann A, Scheja L, Wabitsch M, and Knippschild U. Comparison of fatty acid and gene profiles in skeletal muscle in normal and obese C57BL/6J mice before and after blunt muscle injury. Front Physiol. **9**: 19. 2018. [Medline] [CrossRef]
14. Martins L, Gallo CC, Honda TSB, Alves PT, Stilhano RS, Rosa DS, Koh TJ, and Han SW. Skeletal muscle healing by M1-like macrophages produced by transient expression of exogenous GM-CSF. Stem Cell Res Ther. **11**: 473. 2020. [Medline] [CrossRef]
15. Wang H, Melton DW, Porter L, Sarwar ZU, McManus LM, and Shireman PK. Altered macrophage phenotype transition impairs skeletal muscle regeneration. Am J Pathol. **184**: 1167–1184. 2014. [Medline] [CrossRef]
16. Chiou SH, Chuang MH, Hung CC, Huang HC, Chen ST, Wang KT, and Ho CL. Inhibition of protein kinase C by snake venom toxins: comparison of enzyme inhibition, lethality and hemolysis among different cardiotoxin isoforms. Biochem Mol Biol Int. **35**: 1103–1112. 1995. [Medline]
17. Datta K, Li J, Bhattacharya R, Gasparian L, Wang E, and Mukhopadhyay D. Protein kinase C zeta transactivates hypoxia-inducible factor alpha by promoting its association with p300 in renal cancer. Cancer Res. **64**: 456–462. 2004. [Medline] [CrossRef]
18. Fukawa K, Ito Y, Misaki N, and Bando K. [A new method for the local irritation test. I. Tissue regeneration test for intramuscular acetic acid injection]. Yakugaku Zasshi. **95**: 1307–1316. 1975 (in Japanese). [Medline] [CrossRef]
19. Ochiai T, Matsumoto K, Sekita K, Uchida O, Kawasaki Y, and Furuya T. [Local irritation of isotonic acetic acid solutions of the rabbit M. vastus lateralis and confirmation of the injected sites]. Jikken Dobutsu. **34**: 399–406. 1985 (in Japanese). [Medline]
20. Miller KJ, Thaloor D, Matteson S, and Pavlath GK. Hepatocyte growth factor affects satellite cell activation and differentiation in regenerating skeletal muscle. Am J Physiol Cell Physiol. **278**: C174–C181. 2000. [Medline] [CrossRef]
21. Szade A, Grochot-Przeczek A, Florczyk U, Jozkowicz A, and Dulak J. Cellular and molecular mechanisms of inflammation-induced angiogenesis. IUBMB Life. **67**: 145–159. 2015. [Medline] [CrossRef]
22. Borselli C, Storrie H, Benesch-Lee F, Shvartsman D, Cezar C, Lichtman JW, Vandenburgh HH, and Mooney DJ. Functional muscle regeneration with combined delivery of angiogenesis and myogenesis factors. Proc Natl Acad Sci USA. **107**: 3287–3292. 2010. [Medline] [CrossRef]
23. Yu F, Lin Y, Zhan T, Chen L, and Guo S. HGF expression induced by HIF-1α promote the proliferation and tube formation of endothelial progenitor cells. Cell Biol Int. **39**: 310–317. 2015. [Medline] [CrossRef]
24. Forsythe JA, Jiang BH, Iyer NV, Agani F, Leung SW, Koos RD, and Semenza GL. Activation of vascular endothelial growth factor gene transcription by hypoxia-inducible factor 1. Mol Cell Biol. **16**: 4604–4613. 1996. [Medline] [CrossRef]
25. Wijesundera KK, Izawa T, Tennakoon AH, Golbar HM, Tanaka M, Kuwamura M, and Yamate J. M1-/M2-macrophage polarization in pseudolobules consisting of adipohilin-rich hepatocytes in thioacetamide (TAA)-induced rat hepatic cirrhosis. Exp Mol Pathol. **101**: 133–142. 2016. [Medline] [CrossRef]
26. Nakayama T, Kurobe H, Sugasawa N, Kinoshita H, Higashida M, Matsuoka Y, Yoshida Y, Hirata Y, Sakata M, Maxfield MW, Shimabukuro M, Takahama Y, Sata M, Tamaki T, Kitagawa T, and Tomita S. Role of macrophage-derived hypoxia-inducible factor (HIF)-1α as a mediator of vascular remodelling. Cardiovasc Res. **99**: 705–715. 2013. [Medline] [CrossRef]
27. Armitage P, Berry G, and Matthews JNS. Statistical methods in medical research. John Wiley & Sons, Hoboken. 2008.
28. Rigamonti E, Zordan P, Sciorati C, Rovere-Querini P, and Brunelli S. Macrophage plasticity in skeletal muscle repair. BioMed Res Int. **2014**: 560629. 2014. [Medline] [CrossRef]
29. Bouredji Z, Hamoudi D, Marcadet L, Argaw A, and Frenette J. Testing the efficacy of a human full-length OPG-Fc analog in a severe model of cardiotoxin-induced skeletal muscle injury and repair. Mol Ther Methods Clin Dev. **21**: 559–573. 2021. [Medline] [CrossRef]
30. Qi J, Qiao Y, Wang P, Li S, Zhao W, and Gao C. microRNA-210 negatively regulates LPS-induced production of proinflammatory cytokines by targeting NF-κB1 in murine macrophages. FEBS Lett. **586**: 1201–1207. 2012. [Medline] [CrossRef]
31. Dehne N, Kerkweg U, Flohé SB, Brüne B, and Fandrey J. Activation of hypoxia-inducible factor 1 in skeletal muscle cells after exposure to damaged muscle cell debris. Shock. **35**: 632–638. 2011. [Medline] [CrossRef]
32. Filatova A, Seidel S, Böğürcü N, Gräf S, Garvalov BK, and

Acker T. Acidosis acts through HSP90 in a PHD/VHL-independent manner to promote HIF function and stem cell maintenance in glioma. Cancer Res. **76**: 5845–5856. 2016. [Medline] [CrossRef]
33. Smith TG, Robbins PA, and Ratcliffe PJ. The human side of hypoxia-inducible factor. Br J Haematol. **141**: 325–334. 2008. [Medline] [CrossRef]
34. Jennische E, Ekberg S, and Matejka GL. Expression of hepatocyte growth factor in growing and regenerating rat skeletal muscle. Am J Physiol. **265**: C122–C128. 1993. [Medline] [CrossRef]
35. Tanaka S, Tachino K, Kawahara E, Tanaka J, Funakoshi H, and Nakamura T. Hepatocyte growth factor in mouse soleus muscle increases with reloading after unloading. J Phys Ther Sci. **18**: 33–41. 2006. [CrossRef]
36. Shou J, Shi X, Liu X, Chen Y, Chen P, and Xiao W. Programmed death-1 promotes contused skeletal muscle regeneration by regulating Treg cells and macrophages. Lab Invest. **101**: 719–732. 2021. [Medline] [CrossRef]
37. Wagatsuma A, Tamaki H, and Ogita F. Sequential expression of vascular endothelial growth factor, Flt-1, and KDR/Flk-1 in regenerating mouse skeletal muscle. Physiol Res. **55**: 633–640. 2006. [Medline]
38. Meng XM, Tang PM, Li J, and Lan HY. Macrophage phenotype in kidney injury and repair. Kidney Dis. **1**: 138–146. 2015. [Medline] [CrossRef]
39. Fan ZG, Qu XL, Chu P, Gao YL, Gao XF, Chen SL, and Tian NL. MicroRNA-210 promotes angiogenesis in acute myocardial infarction. Mol Med Rep. **17**: 5658–5665. 2018. [Medline]
40. Tonkin J, Temmerman L, Sampson RD, Gallego-Colon E, Barberi L, Bilbao D, Schneider MD, Musarò A, and Rosenthal N. Monocyte/Macrophage-derived IGF-1 orchestrates murine skeletal muscle regeneration and modulates autocrine polarization. Mol Ther. **23**: 1189–1200. 2015. [Medline] [CrossRef]
41. Kozakowska M, Pietraszek-Gremplewicz K, Ciesla M, Seczynska M, Bronisz-Budzynska I, Podkalicka P, Bukowska-Strakova K, Loboda A, Jozkowicz A, and Dulak J. Lack of heme oxygenase-1 induces inflammatory reaction and proliferation of muscle satellite cells after cardiotoxin-induced skeletal muscle injury. Am J Pathol. **188**: 491–506. 2018. [Medline] [CrossRef]
42. Liu F, Lou YL, Wu J, Ruan QF, Xie A, Guo F, Cui SP, Deng ZF, and Wang Y. Upregulation of microRNA-210 regulates renal angiogenesis mediated by activation of VEGF signaling pathway under ischemia/perfusion injury in vivo and in vitro. Kidney Blood Press Res. **35**: 182–191. 2012. [Medline] [CrossRef]
43. Yang X, Yang S, Wang C, and Kuang S. The hypoxia-inducible factors HIF1α and HIF2α are dispensable for embryonic muscle development but essential for postnatal muscle regeneration. J Biol Chem. **292**: 5981–5991. 2017. [Medline] [CrossRef]
44. Ochoa O, Sun D, Reyes-Reyna SM, Waite LL, Michalek JE, McManus LM, and Shireman PK. Delayed angiogenesis and VEGF production in CCR2-/- mice during impaired skeletal muscle regeneration. Am J Physiol Regul Integr Comp Physiol. **293**: R651–R661. 2007. [Medline] [CrossRef]